Modulated convection at high frequencies and large modulation amplitudes

J. B. Swift
Department of Physics and Center for Nonlinear Dynamics, University of Texas at Austin, Austin, Texas 78712

P. C. Hohenberg
AT&T Bell Laboratories, Murray Hill, New Jersey 07974-2070

(Received 8 July 1987)

Modulated Rayleigh-Bénard convection is analyzed for high frequencies and large modulation amplitudes. The linear theory of Gershuni and Zhukhovitskii is generalized to the nonlinear domain, and a subcritical bifurcation to convection is found in agreement with the experiments of Niemela and Donnelly. The crossover between the high-frequency ("Stokes layer") regime and the low-frequency regime studied previously is analyzed.

I. INTRODUCTION

Rayleigh-Bénard convection under external modulation of the temperature has been studied both theoretically[1–4] and experimentally[5,6] in recent years. In most of this work[1–3,5] the frequency and amplitude of the modulation were assumed not to become too large. More precisely, the relative amplitude of modulation δ was taken to be of order unity or less, so that all interesting effects of modulation were confined to the frequency domain[7] $\omega/\pi^2 \lesssim O(1)$. Recently, Niemela and Donnelly[6] (hereafter referred to as ND) devised an experiment where they modulated a Rayleigh-Bénard cell filled with liquid helium, at dimensionless frequencies[7] of order $\omega/\pi^2 \approx 10$ and relative amplitudes $\delta = O(30)$. These authors pointed out that at such high frequencies convection is confined to a narrow *Stokes layer* of thickness[7]

$$d_s = (2/\omega)^{1/2} \ll 1 , \tag{1.1}$$

which changes the quantitative behavior of the system. The high-frequency situation (1.1) was analyzed by Gershuni and Zhukhovitskii[4] (hereafter referred to as GZ), in a linear theory. They found that for[8] $r_0 = 0$, the critical amplitude was

$$\delta_c \propto \omega^{3/2} , \tag{1.2}$$

a result which was verified by the experiments of ND.

The present paper studies the crossover from the low-frequency large-d_s regime (which is reasonably well described by the Lorenz model of AHL I) to the high-frequency small-d_s regime (1.1). We then generalize the approximate theory of GZ to the nonlinear regime, which allows us to predict the Nusselt number or the temperature difference, and, in particular, to study the nature of the bifurcation to convection (supercritical or subcritical). We find that the crossover from low to high frequency occurs at $\omega \sim \omega_x = 40$, for the Prandtl number of the ND experiment. Our calculations are confined to the case[8] $r_0 = 0$ considered by GZ and ND, but small values of r_0 are not expected to change the situation drastically.

In Sec. II the linear treatment by GZ of the Stokes layer is reviewed and the nonlinear generalization presented and compared with the experiments of ND. We recover a subcritical bifurcation as found experimentally, and correctly predict the position of the saddle-node bifurcation. The jump in temperature at the transition is not obtained with as good accuracy, but the experimental value is difficult to estimate from the results presented by ND. In Sec. III we review the high-frequency behavior of earlier theories of modulated convection, and discuss the crossover from the low- to the high-frequency regimes.

II. SUBHARMONIC BIFURCATION IN THE STOKES LAYER

A. Linear theory

We assume that the bottom plate temperature is modulated, and following GZ we write the temperature as the sum of a conductive and a convective contribution

$$T(\bar{z}) = T_{\rm cond}(\bar{z}) + \theta , \tag{2.1a}$$

$$T_{\rm cond}(\bar{z}) = R_c^{\rm stat}\delta \exp(-\kappa\bar{z})\cos(\kappa\bar{z} - \omega t) , \tag{2.1b}$$

where

$$\kappa = (\omega/2)^{1/2} . \tag{2.1c}$$

Note that in (2.1) we have assumed that the average temperature difference r_0 vanishes.[8] In linear order the velocity and convective contribution to the temperature are, respectively,

$$w = w_l = [w_1(\bar{z})\cos(\omega t/2) + w_2(\bar{z})\sin(\omega t/2)](e^{i\mathbf{k}\cdot\bar{\mathbf{r}}} + \text{c.c.}) \tag{2.2a}$$

and

$$\theta = \theta_l = [\theta_1(\bar{z})\cos(\omega t/2) + \theta_2(\bar{z})\sin(\omega t/2)](e^{i\mathbf{k}\cdot\bar{\mathbf{r}}} + \text{c.c.}) , \tag{2.2b}$$

corresponding to a *subharmonic* bifurcation. As sketched in Appendix A, we insert (2.2) into the

Oberbeck-Boussinesq (OB) equations (A1) and find ordinary differential equations for $w_{1,2}(\bar{z})$ and $\theta_{1,2}(\bar{z})$. These are solved *approximately* by making the ansatz (A2) and determining the unknown constants from boundary conditions and integral relations. The result, shown in Eqs. (A3) and (A4) are precisely those of GZ. In Fig. 1 we show by the solid line the linear threshold (A4) as a function of frequency for a Prandtl number $\sigma=0.49$.

B. Nonlinear theory

We now take solutions of the form

$$w=w_l \ , \tag{2.3a}$$

$$\theta=\theta_l+\theta_0(\bar{z})+\theta_3(\bar{z})\cos(\omega t)+\theta_4(\bar{z})\sin(\omega t) \tag{2.3b}$$

and insert these into the OB equations (A1), keeping only terms with frequencies $\omega,\omega/2$, as well as constant terms. The terms in $\cos(\omega t/2)$ and $\sin(\omega t/2)$ are those of the linear theory which determines the functions $\theta_{1,2}(\bar{z})$ and $w_{1,2}(\bar{z})$ up to a normalization. The terms in $\cos\omega t$ and $\sin\omega t$ lead to equations for $\theta_3(\bar{z})$ and $\theta_4(\bar{z})$ [Eqs. (A10)], which are solved by Laplace transformation. The term independent of t in the equations of motion leads to an equation for $\theta_0(\bar{z})$ of the form

$$\partial_{\bar{z}}\theta_0=L_1(\bar{z})-\langle J\rangle \ , \tag{2.4}$$

where $L_1(\bar{z})$ is given in Eq. (A8) in terms of the linear solutions and $\langle J\rangle$ is the heat current through the fluid, averaged over the lateral coordinates and over time (this average is independent of the vertical coordinate $\bar{z}$). The solution to (2.4) depends on the external constraints on the experiment, which we write, in general, as

$$\langle J^{\rm tot}\rangle=\langle J\rangle-\lambda_w\theta_0(\bar{z}=1)=0 \ , \tag{2.5}$$

where $J^{\rm tot}$ is the total vertical current through the system, the second term is the contribution from the sidewalls, and λ_w is the ratio of conductances of the sidewalls and fluid, respectively. Two special cases of Eq. (2.5) are (i) fixed-zero temperature at the upper plate, which can be achieved by setting $\lambda_w=\infty$ in (2.5), and (ii) fixed-zero current through the fluid, which corresponds to $\lambda_w=0$. A typical experimental situation involves a finite λ_w and Eqs. (2.4) and (2.5) determine the function $\theta_0(\bar{z})$. Equation (2.5) can also be generalized to the case of a nonzero average current $\langle J^{\rm tot}\rangle=J_0$, or average temperature $\theta_0(\bar{z}=1)=R_0$.

The calculations outlined in Appendix A are straightforward but tedious. The final result can be expressed in terms of the average velocity squared ψ^2 and the reduced amplitude

$$\eta=\frac{\delta^2}{\delta_c^2}-1 \tag{2.6a}$$

as

$$\eta=\alpha\kappa^{-6}\psi^2+\beta\kappa^{-12}\psi^4 \ . \tag{2.6b}$$

The linear threshold δ_c is given in (A4), and the coefficients α and β, displayed in (A12), depend on the Prandtl number σ. The main frequency dependence of the result has been scaled out by the factors of $\kappa=(\omega/2)^{1/2}$ appearing in (2.6b) and (A12). When the wall conductance λ_w is zero, α and β are strictly independent of ω, but for finite λ_w a weak frequency dependence remains.

From these results we may predict the Prandtl number σ_t at which the bifurcation changes from subcritical to supercritical, i.e., the "tricritical" value of σ for which $\alpha=0$. For $\lambda_w=0$ we find

$$\sigma_t=4.5 \ . \tag{2.7a}$$

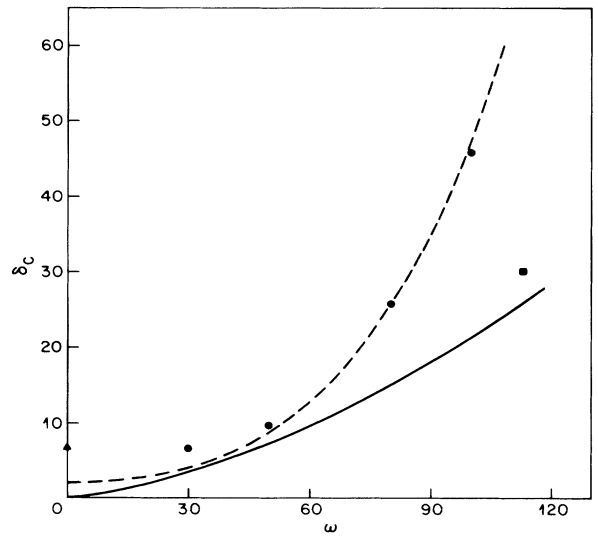

FIG. 1. Linear threshold for onset of modulated convection via a subharmonic bifurcation. The critical amplitude δ_c is plotted as a function of the dimensionless frequency ω, for the case of no average temperature difference ($r_0=0$) and $\sigma=0.49$. The solid line is the result of the "Stokes layer" theory of GZ (Ref. 4), the solid circles come from a numerical evaluation of the Lorenz model of AHL I (Ref. 2), the dashed line is the approximate solution of the Lorenz model discussed in Appendix B, the solid triangle is the exact result of Dowden at $\omega=0$, and the solid square is the experimental result of Niemela and Donnelly (Ref. 6).

C. Comparison with the experiment of Niemela and Donnelly

The experiment of ND corresponds to parameter values $\sigma=0.49$, $\omega=113$, and has a threshold value $\delta_c^{\rm expt}=30.3$, compared to the GZ value $\delta_c^{\rm th}=25.8$. The sidewall thermal conductance corresponds to a value[9] $\lambda_w=0.27$ for which the tricritical σ is

$$\sigma_t=5.5 \ , \tag{2.7b}$$

which means that the bifurcation is expected to be subcritical ($\alpha<0$) for $\sigma=0.49$, with a saddle-node (SN) bifurcation at

$$\delta_{\rm SN}^{\rm th}=0.85\delta_c \ . \tag{2.8}$$

The jump in temperature at $\delta=\delta_c$ turns out to be

$$\left[\frac{\Delta T}{T_{0c}}\right]^{\text{th}}=\frac{\theta_0(\bar{z}=1,\delta=\delta_c)}{\delta_c R_c^{\text{stat}}}=0.058 \tag{2.9a}$$

for $\lambda_w=0$ and

$$\left[\frac{\Delta T}{T_{0c}}\right]^{\text{th}}=0.049 \tag{2.9b}$$

for $\lambda_w=0.27$. To compare to the experimental values[6] we first note that ND modulated the top plate, whereas in our calculation we have assumed modulation of the bottom plate, Eq. (2.1). Tracing through this difference we find that Eq. (2.8) is unchanged, and Eq. (2.9) is reversed in sign. From Fig. 3(a) of ND we find

$$\delta_{\text{SN}}^{\text{expt}}=0.90\delta_c \ , \tag{2.10}$$

and from their Figs. 2 and 3(a) we estimate, at $Ra=Ra_c$,

$$\left[\frac{\Delta T}{T_{0c}}\right]^{\text{exp}}=-0.08\pm0.02 \ . \tag{2.11}$$

Thus the position of the saddle node is correctly obtained by our theory, whereas the magnitude of the jump is somewhat underestimated. (See note added in proof.)

III. DISCUSSION AND CONCLUSION

A. Approximate treatment of the Lorentz model

We may test the approximations made in Sec. II by applying the same procedure to a solution of the Lorenz equations discussed in AHL I. The results for the linear threshold are given in Appendix B and displayed as the dashed line in Fig. 1. The solid points were obtained from a numerical solution of the Lorenz model for rigid boundaries, and correspond to a subharmonic bifurcation. At large ω we find, for $r_0=0$,

$$\left[\frac{\tilde{\delta}_c}{m\omega^2}\right]_{\text{approx}}\sim 0.5 \ , \tag{3.1a}$$

whereas an exact solution of the Lorenz model yields[10]

$$\left[\frac{\tilde{\delta}_c}{m\omega^2}\right]_{\text{exact}}\sim 0.454 \ . \tag{3.1b}$$

The corresponding numbers for a step modulation are 0.375 (approx.) and 0.365 (exact). Thus the ansatz (2.2), (2.3), (A2) works well for the Lorenz model at high frequencies.

B. High- and low-frequency behavior of the OB equations

We may find the high-frequency behavior of the exact second-order threshold formula of Venezian[11] by evaluating the infinite sum over n in his Eq. (45), using an asymptotic formula given by Bender and Orszag.[12] We find

$$r_{0c}=1+(2\sqrt{2}/27)f(\sigma)\delta^2/\omega^{7/2} \ , \tag{3.2}$$

where

$$\begin{aligned} f(\sigma)=(1-\sigma^{-2})^{-3}[&2(\sigma^{-1}+\sigma^{-2})(\sigma^{3/2}-1)\\ &-\tfrac{3}{2}(\sigma^{-1}+\sigma^{-2})(1-\sigma^{-2})\\ &-(\tfrac{21}{16})(1+\sigma^{-1})(1-\sigma^{-2})^2] \ . \end{aligned}$$

The above formula is valid only for δ fixed and $\omega\to\infty$, so it does not apply to the case $r_{0c}\simeq 0$. This formula (3.2) contrasts with the behavior of the Lorenz model for stress-free boundaries in this limit,

$$r_{0c}=1+18\sigma\pi^8\delta^2/\omega^4 \ , \tag{3.3}$$

the difference with (3.2) coming from the higher modes left out of the Lorenz model.

In the limit of zero frequency the threshold was evaluated by Dowden,[13] as discussed in Sec. III C of AHL I. In this limit the Lorenz model is exact for stress-free boundaries and an excellent approximation[2] in the rigid case; the result can be expressed as

$$\tfrac{1}{2}\Gamma=(2\pi)^{-1}\text{Re}\int_0^{2\pi} ds[\epsilon/m+(\Gamma/2)^2+(\delta/m)\cos s]^{1/2} \tag{3.4}$$

in the notation of AHL I, Eq. (B7). For $\sigma=0.49$ and $r_0=0$ we find

$$\delta_c=6.9 \ , \tag{3.5}$$

where we have inserted the parameters m and Γ for the rigid case. This is to be compared with the value $\delta_c=2$ obtained from Eq. (B1) (GZ theory), which is only expected to be correct at high frequencies.

C. Crossover

We have collected the available information on the linear threshold for subharmonic bifurcations in Fig. 1, which plots δ_c versus ω for $r_0=0$ and $\sigma=0.49$. We see that the result based on scaling with the Stokes layer d_s is closest to the Lorenz model result based on scaling with the plate separation $d=1$, for $\omega=\omega_x\approx 40$, i.e., $d_s(\omega)\approx 0.22$. We presume that the correct answer is reasonably well approximated by the GZ (Stokes layer) theory (lower curve) for $\omega>\omega_x$, and by the Lorenz model (solid points) for $\omega<\omega_x$. This assumption is supported by the independent calculation at $\omega=0$ (solid triangle) and by the experimental point at $\omega=113$ (solid square). (See note added in proof.) Moreover, we may test the validity of the Lorenz truncation by considering the extended model of Hohenberg and Swift,[3] which includes the $n=2$ modes left out of the Lorenz model. An evaluation using this model[14] shows that for $\omega=\omega_x$ the $n=2$ modes contribute 20% to the average Nusselt number. For $\omega<\omega_x$ the contribution is smaller, but it becomes of order unity when $\omega\gg\omega_x$. Thus it is reasonable to infer that the Lorenz formulas (based on scaling on the length d) can be trusted for $\omega<\omega_x$, but not for $\omega>\omega_x$.

Finally we comment on the question of the correct convective pattern in the high-frequency regime. Niemela and Donnelly interpreted their subcritical bifurcation as possible evidence for a hexagon pattern, as discussed by Roppo *et al.*[15] and the present authors.[3] Our

crude theory presented in Sec. II is based on a roll pattern and it yields a subcritical bifurcation, as discussed above. Indeed, the Lorenz model itself has a subcritical bifurcation for $\omega=113$.[16,14] Thus the subcritical bifurcation does not represent evidence, one way or the other, for a hexagon pattern. The extended Lorenz model of Ref. 3 which includes hexagons can also be solved numerically for the parameters of ND, but since the contribution of the $n=2$ modes turns out[14] to be as large as that of the fundamental ($n=1$) mode, it is clear that the theory is unreliable. This is to be expected since the conductive profile is very far from linear in the high-frequency limit. We therefore conclude that the nature of the convection pattern cannot be determined in this regime by the theories we have discussed in the present paper, and a better calculation is called for to resolve this issue. We expect, however, that the position of the saddle node and the order of magnitude of the temperature jump at the bifurcation will not depend too much on the nature of the convective pattern.

Note added in proof. Further analysis by ND of unpublished data in addition to those in Fig. 3(a) gives average values $\delta_{\rm SN}^{\rm expt}/\delta_c=0.86$ and $[\Delta T/T_{0c}]^{\rm expt}=-0.066$, respectively, which improve the agreement between experiment and theory.

Subsequent analysis of unpublished data by ND at lower frequencies lends support to a crossover at $\omega_x\approx 40$. For frequencies just below the crossover the data agree with the numerical Lorenz-model result, but at a still lower frequency ($\omega=18$) the data fall below the Lorenz-model value. The reason for this discrepancy is not known at the present time.

ACKNOWLEDGMENTS

The authors are pleased to acknowledge useful conversations with G. Ahlers, R. J. Donnelly, W. D. McCormick, and J. J. Niemela, and computational assistance from D. Barkley. One of us (J.B.S.) wishes to thank AT&T Bell Laboratories for its hospitality during part of this work, as well as the U.S. Department of Energy for partial support (under Contract No. DE-AS05-84ER13147).

APPENDIX A

The hydrodynamic equations, in the Oberbeck-Boussinesq (OB) approximation, may be written as[2,14]

$$\tilde{\nabla}^2\partial_t w=\sigma\tilde{\nabla}^4 w+\sigma\nabla^2\theta+\bar{T}\ , \tag{A1a}$$

$$\partial_t\theta=\tilde{\nabla}^2\theta-w\partial_z T_{\rm cond}-\tilde{V}\cdot\tilde{\nabla}\theta\ , \tag{A1b}$$

$$\bar{T}=\hat{\bar{z}}\cdot\tilde{\nabla}\times\tilde{\nabla}\times(\tilde{\nabla}\cdot\tilde{\nabla}\tilde{\nabla})\ , \tag{A1c}$$

$$\tilde{\nabla}\cdot\mathbf{V}=0\ , \tag{A1d}$$

where $T_{\rm cond}$ is given in Eq. (2.1), σ is the Prandtl number, and we use the notation $\tilde{\nabla}=(\nabla,\partial_{\bar{z}})$, where ∇ is the horizontal Laplacian, $\tilde{\mathbf{V}}=(\mathbf{u},w)$ is the velocity, $\bar{z}$ is the vertical coordinate, and the units[7] are those of AHL I.

1. Linear theory

We neglect the nonlinear terms, insert (2.1) and (2.2) into (A1), and find ordinary differential equations for $w_{1,2}(\bar{z})$ and $\theta_{1,2}(\bar{z})$. We follow GZ (Ref. 4) and solve these equations approximately making the ansatz

$$w_{1,2}(\bar{z})=\bar{w}_{1,2}F(\bar{z})\ , \tag{A2a}$$

with

$$F(\bar{z})=\bar{z}^2e^{-a\bar{z}} \tag{A2b}$$

and

$$\theta_{1,2}=\bar{\theta}_{1,2}\Phi(\bar{z})\ , \tag{A2c}$$

with

$$\Phi(\bar{z})=(\bar{z}+a\bar{z}^2)e^{-a\bar{z}}\ , \tag{A2d}$$

for rigid boundary conditions. The unknowns are the constants $\bar{w}_{1,2},\bar{\theta}_{12}$ (not determined at linear order) and the constants a and k. The critical value $\delta_c(a,k,\sigma)$ is determined by substituting (A2) into the ordinary differential equation obtained from (A1), (2.1), and (2.2). We find

$$\begin{bmatrix}\delta I_- -B & \delta I_+ +A\\ -\delta I_+ +A & \delta I_- +B\end{bmatrix}\begin{bmatrix}\bar{w}_1\\ \bar{w}_2\end{bmatrix}=\begin{bmatrix}0\\0\end{bmatrix}\ , \tag{A3a}$$

where

$$A=(\tfrac{1}{4}\omega^2K_0J_1-\sigma K_1J_2)/(\sigma k^2K_0)\ , \tag{A3b}$$

$$B=\tfrac{1}{2}\omega(K_1J_1+\sigma K_0J_2)/(\sigma k^2K_0)\ , \tag{A3c}$$

$$I_\pm=R_c^{\rm stat}\int_0^\infty d\bar{z}(\kappa/2)e^{-\kappa\bar{z}}[\cos(\kappa\bar{z})\pm\sin(\kappa\bar{z})]F(\bar{z})\ , \tag{A3d}$$

with

$$J_n=\int_0^\infty(\partial_{\bar{z}}^2-k^2)^nF(\bar{z})d\bar{z} \tag{A3e}$$

and

$$K_n=\int_0^\infty(\partial_{\bar{z}}^2-k^2)^n\Phi(\bar{z})d\bar{z}\ . \tag{A3f}$$

Equations (A3) yield

$$\delta_c^2=\left[\frac{2\kappa^6[(1+\tilde{a})^2+1]^3}{9(R_c^{\rm stat})^2\sigma^2\tilde{k}^4\tilde{a}^6}\right]\times[(3\tilde{k}^2-\sigma I_1I_2)^2+(3\sigma I_1+\tilde{k}^2I_2)^2]\ , \tag{A4}$$

where $a=\kappa\tilde{a}$, $k=\kappa\tilde{k}$, $I_2=\tilde{a}^2+3\tilde{k}^2$, $I_1=\tilde{k}^4+3\tilde{a}^4$, and $\tilde{a}$ and $\tilde{k}$ are determined by minimizing (A4) with respect to $\tilde{a}$ and $\tilde{k}$.

2. Nonlinear theory

As explained in Sec. II, Eqs. (2.3) and (A1) lead to the equation for $\theta_0(\bar{z})$,

$$\partial^2\theta_0(\bar{z})=\tilde{\psi}^2\partial g(\bar{z})\ , \tag{A5a}$$

where

$$\tilde{\psi}^2=\bar{w}_1\bar{\theta}_1+\bar{w}_2\bar{\theta}_2 \tag{A5b}$$

and

$$g(\bar{z})=F(\bar{z})\Phi(\bar{z}) \tag{A5c}$$

(we here use the notation $\partial\equiv\partial_{\bar{z}}$). It follows that

$$\theta_0(\bar{z})=\tilde{\psi}^2\int_0^{\bar{z}} g(\bar{z}')d\bar{z}'+c_1\bar{z} \ . \tag{A6}$$

The integration constant c_1 is related to the average current, $\langle J\rangle$ (averaged over horizontal coordinates and time) by using Eq. (A26) in AHL I, as well as (2.2) and (2.3). We find

$$\langle J\rangle=-\partial\theta_0+\tilde{\psi}^2 g=-c_1 \ . \tag{A7}$$

This gives (2.4) with

$$L_1(\bar{z})=\tilde{\psi}^2 g(\bar{z}) \ . \tag{A8}$$

For the boundary condition (2.5) we thus have

$$\langle J\rangle=(9/8a^4)\lambda_w(1+\lambda_w)^{-1}\tilde{\psi}^2 \tag{A9a}$$

and

$$\theta_c(\bar{z}=1)=(9/8a^4)(1+\lambda_w)^{-1}\tilde{\psi}^2 \ . \tag{A9b}$$

The equations for θ_3 and θ_4 are

$$-\omega\theta_3(\bar{z})=\partial^2\theta_4-(\bar{w}_1\bar{\theta}_2+\bar{w}_2\bar{\theta}_1)\partial g(\bar{z}) \tag{A10a}$$

and

$$\omega\theta_4(\bar{z})=\partial^2\theta_3-(\bar{w}_1\bar{\theta}_1-\bar{w}_2\bar{\theta}_2)\partial g(\bar{z}) \ , \tag{A10b}$$

which can be solved by Laplace transforms. We now insert θ_3, θ_4, and θ_0 back into the equations for $\theta_{1,2}$ and $w_{1,2}$ keeping only the subharmonic terms $[\cos(\omega t/2),\sin(\omega t/2)]$, and integrate over $\bar{z}$. As a result Eq. (A3) is changed to

$$\begin{bmatrix} \delta I_- -B-B'\psi^2 & \delta I_+ +A+A'\psi^2 \\ -\delta I_+ +A+A'\psi^2 & \delta I_- +B+B'\psi^2 \end{bmatrix}\begin{bmatrix}\bar{w}_1\\ \bar{w}_2\end{bmatrix}=\begin{bmatrix}0\\0\end{bmatrix} \ , \tag{A11a}$$

where

$$\psi^2=\bar{w}_1^2+\bar{w}_2^2=(k^2K_0/J_2)\tilde{\psi}^2 \ , \tag{A11b}$$

$$A'=(P\sigma J_2+\omega QJ_1/2)/(\sigma k^2K_0)+J_2n_0/k^2K_0 \ , \tag{A11c}$$

$$B'=(\sigma J_2Q-\tfrac{1}{2}\omega PJ_1)/(\sigma k^2K_0) \ , \tag{A11d}$$

$$n_0=(2/a^3)(\tilde{c}_1+20/81a^3) \ , \tag{A11e}$$

$$c_1=\tilde{c}_1\tilde{\psi}^2 \ , \tag{A11f}$$

$$P=-\tfrac{1}{2}\kappa^{-6}(P_1+P_2) \ , \tag{A11g}$$

$$Q=-\tfrac{1}{2}\kappa^{-6}(Q_1+Q_2) \ , \tag{A11h}$$

$$P_1=(27)^{-1}(40h_1/3\tilde{a}^6+216h_2/9\tilde{a}^5+22h_3/\tilde{a}^4+10h_4/\tilde{a}^3+2h_5/\tilde{a}^2) \ , \tag{A11i}$$

$$h_1=4\tilde{a}^4\tilde{a}_1 \ ,$$

$$h_2=-8\tilde{a}^3\tilde{a}_1^2 \ ,$$

$$h_3=4\tilde{a}^2(3-20\tilde{a}^4)\tilde{a}_1^3 \ ,$$

$$h_4=-12\tilde{a}(8\tilde{a}^8-40\tilde{a}^4+1)\tilde{a}_1^4 \ ,$$

$$h_5=-6(35\times2^6\tilde{a}^{12}-2^4\times155\tilde{a}^8+260\tilde{a}^4-1)\tilde{a}_1^5 \ ,$$

$$\tilde{a}_1=(4\tilde{a}^4+1)^{-1} \ ,$$

$$\begin{aligned}P_2=-(1+x^2)^{-3}(1+y^2)^{-4}\{&6[(x^3-3x^2-3x+1)(y^4-6y^2+1)-(x^3+3x^2-3x-1)(4y^3-4y)]\\&+24\tilde{a}(1+y^2)^{-1}[(x^3-3x^2-3x+1)(y^5-10y^3+5y)\\&-(x^3+3x^2-3x-1)(5y^4-10y^2+1)]\}\end{aligned} \tag{A11j}$$

$$x=-1-\tilde{a} \ , \tag{A11k}$$

$$y=2\tilde{a}-1 \ ,$$

$$Q_1=-(27)^{-1}(40h_6/3\tilde{a}^6+216h_7/9\tilde{a}^5+22h_8/\tilde{a}^4+10h_9/\tilde{a}^3+2h_{10}/\tilde{a}^2) \ , \tag{A11l}$$

$$h_6=2\tilde{a}^2\tilde{a}_1 \ ,$$

$$h_7=-2\tilde{a}(1-4\tilde{a}^4)\tilde{a}_1^2 \ ,$$

$$h_8=(48\tilde{a}^8-48\tilde{a}^4+1)\tilde{a}_1^3 \ ,$$

$$h_9=24\tilde{a}^3(16\tilde{a}^8-40\tilde{a}^4+5)\tilde{a}_1^4 \ ,$$

$$h_{10}=12(5\times2^6\tilde{a}^{12}-101\times2^6\tilde{a}^8+135\times2^2\tilde{a}^4-15)\tilde{a}_1^5 \ , \tag{A11m}$$

and

$$Q_2=-(1+x^2)^{-3}(1+y^2)^{-4}\{6[x^3+3x^2-3x-1)(y^4-6y^2+1)+(x^3-3x^2-3x+1)(4y^3-4y)]$$
$$+24\bar{a}(1+y^2)^{-1}[(x^3+3x^2-3x-1)(y^5-10y^3+5y)$$
$$+(x^3-3x^2-3x+1)(5y^4-10y^2+1)]\} \ . \tag{A11n}$$

Equations (A11) yield (2.6) with α and β given by

$$\alpha=2\kappa^6(BB'+AA')/(A^2+B^2) \ , \tag{A12a}$$

$$\beta=\kappa^{12}(A'^2+B'^2)/(A^2+B^2) \ . \tag{A12b}$$

APPENDIX B

In this appendix we apply the GZ approximations used in Appendix A to the Lorenz model given in Eq. (2.7) of AHL I.

1. Linear theory

Using the ansatz (2.2) we obtain

$$\delta_c^2=(A^2+B^2)/(I_+^2+I_-^2) \ , \tag{B1a}$$

where in the notation of AHL I

$$A=1-(\omega\tau_1/2)^2\tilde{\sigma}^{-1} \ , \tag{B1b}$$

$$B=(\tfrac{1}{2}\omega\tau_1)(1+\tilde{\sigma}^{-1}) \ , \tag{B1c}$$

and for free boundary conditions

$$I_+^2+I_-^2=\tfrac{1}{4}[1+(\omega/4\pi^2)^2]^{-1} \ , \tag{B1d}$$

while for rigid boundary conditions

$$I_+^2+I_-^2=F_1F_2/4 \ , \tag{B1e}$$

with

$$F_1=[1+(\omega/\pi^2)^2]^{-1}[1+(\omega/9\pi^2)^2]^{-1} \tag{B1f}$$

and

$$F_2=\frac{2\mu^2(\sinh^2\mu\cosh^2\mu+\sin^2\mu\cos^2\mu)}{(\cos^2\mu\sinh^2\mu+\sin^2\mu\cosh^2\mu)^2} \ , \tag{B1g}$$

with $\mu=\sqrt{\omega/8}=\kappa/2$.

2. Nonlinear theory

In the lowest nonlinear order we obtain

$$\eta=\alpha\psi^2+\beta\psi^4 \ , \tag{B2}$$

where $\psi^2=x_1^2+x_2^2$, the constants x_1 and x_2 are the expansion coefficients of $x(t)$ in terms of $\cos(\omega t/2)$ and $\sin(\omega t/2)$, η is given in (2.6a), and α and β are given by expressions of the form (A12) with $\kappa=1$ and

$$A'=\tfrac{1}{2}\left[1+\frac{1+\omega^2\tau_1^2/2\tilde{\sigma}b}{1+(\omega\tau_1/b)^2}\right] \ , \tag{B3a}$$

$$B'=-\tfrac{1}{2}\omega\tau_1[1/2\tilde{\sigma}-1/b]/[1+(\omega\tau_1/b)^2] \ , \tag{B3b}$$

using the notation of AHL I.

[1]S. H. Davis, Annu. Rev. Fluid Mech. **8**, 57 (1976).

[2]G. Ahlers, P. C. Hohenberg, and M. Lücke, Phys. Rev. A **32**, 3493 (1985), hereafter referred to as AHL I.

[3]P. C. Hohenberg and J. B. Swift, Phys. Rev. A **35**, 3855 (1987).

[4]G. Z. Gershuni and E. M. Zhukhovitskii, *Convective Stability of Incompressible Fluids,* translated by D. Louvish (Keter, Jerusalem, 1976), hereafter referred to as GZ.

[5]G. Ahlers, P. C. Hohenberg, and M. Lücke, Phys. Rev. A **32**, 3519 (1985).

[6]J. J. Niemela and R. J. Donnelly, Phys. Rev. Lett. **57**, 583 (1986), hereafter referred to as ND.

[7]Throughout this paper we use dimensionless units such that length, time, speed, pressure, and temperature are scaled according to the units d, d^2/K, K/d, ρ_0K^2/d^2, and $K\nu/\alpha gd^3$, respectively, where d is the plate spacing, K is the thermal diffusivity, α the thermal expansion, ν the kinematic viscosity, ρ_0 the average density, and g the acceleration of gravity. The vertical coordinate is $\bar{z}$, with $\bar{z}=0$ and 1 at the lower and upper plates, respectively.

[8]Following AHL I we write the temperature difference between the lower and upper plates as $\Delta T(t)/R_c^{\rm stat}=R(t)/R_c^{\rm stat}=r_0+\delta\cos\omega t$, where $R_c^{\rm stat}$ is the critical Rayleigh number in the absence of modulation. Niemela and Donnelly (Ref. 6) define a Rayleigh number $N_{\rm Ray}=Ra\equiv g\alpha T_0d_s^3/K\nu$, where T_0 is the amplitude of temperature modulation. The relation between δ and $N_{\rm Ray}$ is thus $\delta=N_{\rm Ray}/d_s^3R_c^{\rm stat}=N_{\rm Ray}\omega^{3/2}/2\sqrt{2}R_c^{\rm stat}$.

[9]J. J. Niemela and R. J. Donnelly (private communication).

[10]As explained in AHL I the linear threshold is given by a damped Hill's equation [Eq. (B3)]. For high frequency we have $a=0$ in (B3) and the eigenvalue $q=2\tilde{\delta}/m\omega^2=0.908$, corresponding to a subharmonic bifurcation, is found from the quantity $b_1(q)$ given on p. 724 of *Handbook of Mathematical Functions,* edited by M. Abramowitz and I. A. Stegun (Dover, New York, 1965). This value of q leads to Eq. (3.1b) of the text, with $\tilde{\delta}$ related to δ by Eq. (3.6d) of AHL I, with $\bar{\Delta}(\omega)=9\pi^4\gamma\Delta\,[2\tan(\gamma/2)(\pi^2-\gamma^2)(9\pi^2-\gamma^2)]^{-1}$ in place of Eq. (2.32e) which has a misprint.

[11]G. Venezian, J. Fluid Mech. **35**, 243 (1969).

[12]C. M. Bender and S. A. Orszag, *Advanced Mathematical Methods for Scientists and Engineers* (McGraw-Hill, New York, 1978), p. 303.

[13]J. Dowden, J. Fluid Mech. **110**, 149 (1981).

[14]J. B. Swift and P. C. Hohenberg (unpublished).

[15]M. N. Roppo, S. H. Davis, and S. Rosenblat, Phys. Fluids **27**, 796 (1984).

[16]G. Ahlers (private communication).